



ISSN: 2617-6548

URL: www.ijirss.com

Experimental study of a temperature measurement system for an overhead power line using sensors based on TFBG

 Aliya Kalizhanova¹,  Murat Kunelbayev^{2*},  Waldemar Wojcik³,  Ainur Kozbakova⁴

¹*Institute of Information and Computational Technologies CS MSHE RK, Almaty University of Energy and Communications named after G. Daukeyev, Kazakhstan.*

²*Institute of Information and Computational Technologies CS MSHE RK, Kazakhstan.*

³*Lublin Technical University, Poland.*

⁴*Institute of Information and Computational Technologies CS MSHE RK, Almaty Technological University, Kazakhstan.*

Corresponding author: Murat Kunelbayev (Email: murat7508@yandex.kz)

Abstract

This article presents the use of an inclined fiber sensor Bragg grid to control the extension of wires in overhead lines. An aspect of the technological novelty of the project is the development of an innovative optoelectronic system for monitoring and diagnosing the condition of building structures based on a combination of conventional Bragg gratings. The lighting power sensor is installed directly on the controlled transmission of the power line in the form of fittings with a copper plate. A photosensitive multimode optical fiber is attached to the copper plate, at the end of which an inclined fiber Bragg grating is fixed, connected to a multimode optical fiber using a fiber-optic connector through an optical connector. An ultraviolet excimer laser and a light power detector are connected to a fiber-optic connector. The study showed that by selecting the appropriate mechanical parameters of the extension transformer, taking into account the optical parameters of the sensor, and using a special filter, the optical-mechanical system can be configured in the required range to control the sagging of the overhead line wire. During measurements to simulate the operation of a power line wire, the temperature was forced to vary in the range of 10-60°C. This led to the lengthening of the test wire from 38.987 m to 49.275 m; the error was within 4%. The deflection range depends on the distance between the supports, the type of wire, and its actual length in the span, which actually determines the deflection.

Keywords: Bragg gratings, Cable, Fiber-optic sensor, Light power detector, Optoelectronic system, Temperature, Ultraviolet excimer laser.

DOI: 10.53894/ijirss.v7i1.2596

Funding: This research is supported by the Ministry of Science and Higher Education of the Republic of Kazakhstan (Grant number: AP09259547 and AP19679153).

History: Received: 25 August 2023/**Revised:** 3 October 2023/**Accepted:** 12 December 2023/**Published:** 18 January 2024

Copyright: © 2024 by the authors. This article is an open access article distributed under the terms and conditions of the Creative Commons Attribution (CC BY) license (<https://creativecommons.org/licenses/by/4.0/>).

Authors' Contributions: All authors contributed equally to the conception and design of the study. All authors have read and agreed to the published version of the manuscript.

Competing Interests: The authors declare that they have no competing interests.

Transparency: The authors confirm that the manuscript is an honest, accurate, and transparent account of the study; that no vital features of the study have been omitted; and that any discrepancies from the study as planned have been explained. This study followed all ethical practices during writing.

Institutional Review Board Statement: The Ethical Committee of the Institute of Information and Computational Technologies CS MSHE RK, Kazakhstan has granted approval for this study.

Publisher: Innovative Research Publishing

1. Introduction

Currently, electricity is important for the functioning of large enterprises and urban agglomerations, as well as for urban consumers living both in cities and in agricultural areas. In [Zygarlicki and Mroczka \[1\]](#) and [Terzija and Stanojevic \[2\]](#), an analysis of how electric power companies are required to guarantee conventional power supply with regulatory parameters is considered. The measurement of the extension of the power line cable is connected with the calculation of sagging, which seems to be an unsafe parameter for the safe operation of a high-voltage power line. In [Black and Chisholm \[3\]](#) and [Lovrenčić, et al. \[4\]](#), commercially inexpensive deflection reduction technologies have been developed and studied. In the article [Conductor Working Group P738 \[5\]](#) and [CIGRE Working Group 22.12 \[6\]](#), calculations of sagging wires were considered in two stages; the first step was to establish the temperature of the wires using thermal models, weather criteria, and current measurements, and the second stage was calculations of automatic sagging; voltage was studied based on the technical parameters of the power line device [7]. In [Wydra, et al. \[8\]](#), a system was used to measure weather and voltage, as well as establish video surveillance using a video camera. Using a system based on fiber Bragg gratings, they can be used for automatic measurement of all kinds of quantities, such as deformation [9], circulation and twisting [10, 11], bending [12], or curvature [13]. There are many concepts of signal polling using fiber converters with a Bragg lattice [14-16]. In [Crunelle, et al. \[17\]](#) and [Liu, et al. \[18\]](#), controlled deformation was investigated using a filter grating, i.e., piezoelectric drives, until the Bragg wavelengths of both gratings overlapped. In [Lloyd, et al. \[19\]](#), several Bragg sensors on the same fiber were used. The design enables you to set the wavelength of the light that the corresponding measuring component reproduces. A position was created in the article [20] for estimating deflection using a pilot plant with gratings that have an uneven period. It was suggested that that uniform Bragg gratings could be used as both elongation sensors and optical filter structure. In measuring systems, the measured value naturally activates the shift of the main Bragg wavelength of FBG sensors. In [Ribeiro, et al. \[21\]](#), a demodulation technique based on the matched filter method was investigated, in which the requesting array has the same spectral shape as the sensor array. As a rule, such a design can be implemented in the reflection or transmission mode. In [Davis and Kersey \[22\]](#) and [Wade, et al. \[23\]](#), an optical transmission design was developed in which only one (touch) recreates the radiation, and the requesting grid is represented as a filter blocking this radiation. As a result, when the centers of the gratings with Bragg wavelengths coincide, the minimum number of emissions reaches the detector. When the wavelength of the sensitive matrix is shifted, the radiation reaching the detector increases. In both variants, the so-called filter interaction means that the spectral characteristics of both lattices are similar or at least have the same bandwidth [24]. In the works [Fallon, et al. \[25\]](#) and [Zhang, et al. \[26\]](#), chirped gratings were used, where, in addition, the systems allow to increase the measurement spectrum and exclusively increase the rectilinear characteristic of the transient process. In addition, there are systems in which the filtering subject has a significantly larger spatial spectrum than the FBG sensor, and it is also likely to compose the spectrum of the radiation source itself [27]. The article [Garção, et al. \[28\]](#) presents the use of a Bragg grid sensor with a polling system to control the extension of overhead power line wires.

The purpose of this work is to create a system for measuring temperature and extending the cable of an overhead power line, which allows measurements to be carried out with minimal energy consumption. The study used an inclined fiber Bragg grating on the control board, which was characterized by a slight shift in the spectra with a clear coincidence.

2. Materials and Methods

Calculations of tension near the sag are made using only the horizontal component of the tension H ; however, the average value of the horizontal tension and the tension at the fulcrum F is naturally indicated (1). The right part of [Equation 1](#) corresponds to a parabolic approximation of a continuous function.

$$L = \frac{2H}{w} \sinh h\left(\frac{Sw}{2H}\right) = S\left(1 + \frac{S^2 w^2}{24H^2}\right) \quad (1)$$

The total length of the wire can possibly be formulated as a function of D , as represented in [Equation 2](#):

$$L = S + \frac{8D^2}{3S} \quad (2)$$

Using [Equation 2](#), we can write the formula for the relationship between conductor sag D versus span length and conductor length L as shown below:

$$D = \sqrt{\frac{3S(L-S)}{8}} \quad (3)$$

The difference between the length of the conductor L and the length of the span is determined by the deflection of the wire. [Equation 3](#) shows that non-significant changes in sag lead to significant changes in conductor sag. As mentioned above, the deflection of the wire depends in a key way on the overall length of the conductor L when the length of the span remains constant. The temperature dependence of the length L of the conductor is naturally calculated using [Equation 4](#):

$$L_2 = \alpha_{AS} L_1 (T_2 - T_1) + \beta L_1 (\sigma_2 - \sigma_1) \quad (4)$$

Where indices 1 and 2 are the initial and final states, respectively; L_1 , L_2 is the wire length, T_1 , T_2 is the wire temperature; α - coefficient of thermal elongation; σ_1 , σ_2 is the voltage in the conductor; and β is the coefficient of elastic elongation of the wire.

The calculation of the temperature-stressed state of the span of the power line is made using Equation 5 and is solved using repeated methods

$$\sigma^2 - \frac{S^2 g^2}{24\beta\sigma_1^2} = \sigma_1 - \frac{S^2 g^2}{24\beta\sigma_1} - \frac{\alpha}{\beta}(T_2 - T_1) \tag{5}$$

Where S is the span length; $\sigma_1, \sigma_2 = H/A$, stress in the wire; $g = w/A$, bulk density; A is the cross-sectional area of the wire, and $\beta = 1/\gamma$ is the coefficient of elastic elongation of the wire. For VVG wire $\alpha = 16.2 \times 10^{-6} \text{ 1/K}$, $\gamma = 54,000 \text{ MPa}$, $A = 200.7 \text{ mm}^2$, $w = 9.52 \text{ N/m}$, and $g = 30.50 \text{ N/(m mm}^2)$.

This paper presents a direct method for calculating the deflection D, made by measuring the elongation of the conductor in one place with the support of the FBG sensor. If the horizontal stretch H and the thermal stretch of the conductor stay the same throughout the span, measuring the nominal elongation of Δl of a 10 cm long piece of wire gives you the information you need to figure out the total length L of the wire, as shown in Equations 6–9. According to the previous judgments, the comparative wire stretch Δl may exist predetermined depending on the sensor range width, as shown below.

$$\Delta l = C_{OP1} * \Delta FWHM_{FBG} \tag{6}$$

$$E = \frac{\Delta l}{l_{ref}} = \frac{C_{OP1} * \Delta FWHM_{FBG}}{l_{ref}} \tag{7}$$

Where E is the elongation factor as a measured function of the full width half maximum; COP1 is the experimentally estimated coefficient of sensitivity of the elongation sensor; l_{ref} is the reference distance between the installed sensor clamps on the conductor; and Δl is the extension of the wire segment enclosed by the sensing head and measured by the FBG:

$$L = L_{ref} (1 + E) \tag{8}$$

Assuming the above (Equation 8), the connection of the conductor sag D (Equation 3) gives us the following character:

$$D = \sqrt{\frac{3S(L_{ref}(1 + E) - S)}{8}} \tag{9}$$

According to Equations 3 and 8, it is shown that to calculate the sagging of the wire, it is sufficient to set the tension of the conditioned section of the wire.

The research and the development of the system for measuring temperature and the length of an overhead power line’s cable is described in this article. The system has to show how likely it is that changes in the optical parameter s of a sensor with an inclined fibre Bragg grid on the control board will lead to changes in radiation power. The presented design appears to be part of a single system that has been studied and that will determine both the lengthening and the temperature of the power line. This will allow you to imagine the bending of wires that happens during operation in conditions of catastrophic icing and overload of the power line. The use of both temperature and conductor elongation measurements ensures that the acquired totals appear redundant.

Figure 1 shows a test bench used to measure the sag of a power line wire using a real power line.

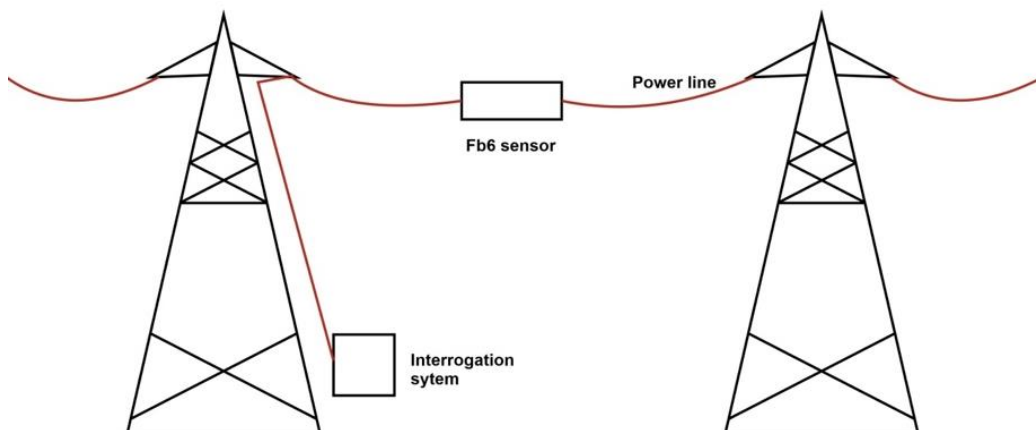


Figure 1. Experimental bench used to measure the sag of a power line wire using a real power line.

The scientific novelty of this system of temperature measurement and extension of the overhead power line cable includes: fittings, inclined fiber Bragg grating on the control board, multimode optical fiber, optical coupling, ultraviolet excimer laser, and fiber optic connector. The light power sensor is installed directly on the controlled transmission of the power line in the form of fittings with a copper plate. A photosensitive multimode optical fiber is attached to the copper plate, at the end of which an inclined fiber Bragg grating is fixed, connected to a multimode optical fiber using a fiber optic

connector through an optical connector. An ultraviolet excimer laser and a light power detector are connected to a fiber-optic connector.

The theoretical significance of the research provided is the applicability of the constructed system for predicting the sagging of power transmission lines, which can be useful for technical support of power transmission and distribution lines, reducing capacity with proper control, increasing the productivity of the electric network and the benefits of higher energy efficiency, as well as for calculating investments in energy infrastructure and large-scale, scalable energy sources.

The research is useful because it led to the creation of a fiber-optic sensor with an inclined Bragg lattice that shows a slight shift in the spectra. It was found that the transition property has a regular response associated with the central Bragg peak and a nonlinear range with a saturation slope conjugated with side bands on the closer side. The research showed that the opt mechanical state could be changed to fit the needed deviation observation range by shifting the advantage to the mechanical parameters of the elongation convertor and the optical adjustment parameters. The difference in range depends on the distance between the poles and the best length of the power line cable. The developed method makes it possible to significantly improve the output parameters of the sensor and reduce the cost by simplifying the setup and testing process. All this indicates a deep study of the theoretical and practical aspects of this study.

The temperature measurement and wire extension system are mounted on a copper or aluminum cable of electric transmission line 1, which consists of two fittings. There are grooves 3 in the fittings, in which a copper plate 4 with a certain length is stuck. The copper plate 4 has a hole 5 in which epoxy resin 6 is poured. An inclined fiber Bragg grating 7 is attached to the copper plate 4 with epoxy resin, which is recorded on a multimode optical fiber 8. An optical sleeve 9 is attached to the multimode optical fiber to provide free tension and extension of the measuring system. Light from the ultraviolet excimer laser 10 enters the fiber optic connector 11, then enters the light power detector 12, where the temperature and cable elongation are measured.

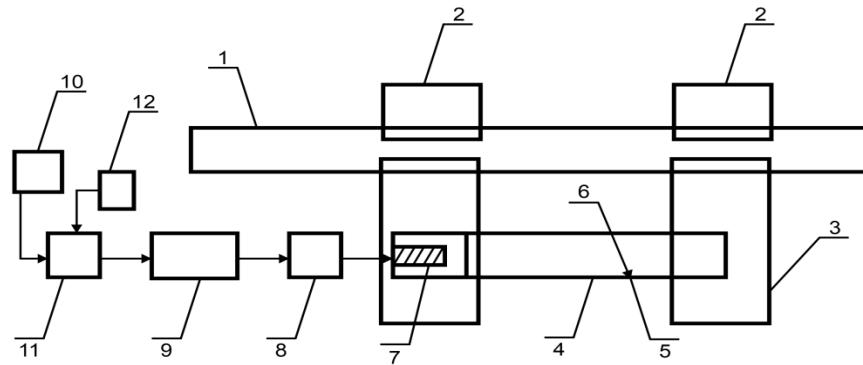


Figure 2. Overhead power line temperature measurement and cable extension system.

Figure 2 illustrates a system for measuring the temperature of an overhead power line and cable extension.

3. Results

The lattice planes are subject to thermal and mechanical disturbances. Since glass is subject to thermal and mechanical influences, so are the gratings recorded on it. When the external action changes, the phase-matching condition changes, which leads to a rearrangement of the reflection wavelength. Thus, by tracking the wavelength at which the Bragg reflection occurs, one can obtain the magnitude of the external disturbance. This functionality fulfills the purpose of fiber optic sensors: to have a structure on the fiber core that provides an absolute reading mechanism. The resonant wavelength λ_{BG} depends on the temperature of the fiber and on the mechanical tensile or compressive stresses applied to it. This circumstance underlies the use of FBGs as sensitive elements of sensors of physical, chemical, and other quantities. The FBG resonance is found by looking at the central wavelength of the radiation that is reflected back from the Bragg grating (BG). This wavelength is affected by the core's effective refractive index (ERI) and the grating period. Mechanical and thermal changes will have an impact on EPP as well as the periodic distance between the lattice planes. These influences are, in turn, the basis for the use of fiber Bragg gratings for voltage and temperature measurements. Using the first-order Bragg condition, we obtain the shift of the resonant wavelength due to mechanical and thermal changes:

$$\Delta\lambda_{BG} = 2\left(\Lambda \frac{\partial n_{eff}}{\partial l} + n_{eff} \frac{\partial \Lambda}{\partial l}\right)\Delta l + 2\left(\frac{\partial n_{eff}}{\partial T} + n_{eff} \frac{\partial \Lambda}{\partial T}\right)\Delta T \quad (10)$$

The first term in Equation 10 describes the effect of tensile strain on an optical fiber. It is responsible for changing the space between the BG planes and for the mechano-optical change in the refractive index (RI). This term can be written as follows:

$$\Delta\lambda_{BG} = \lambda_{BG} \left\{ 1 - \left[\frac{n_{eff}^2}{2} (p_{12} - \nu(p_{11} + p_{12})) \right] \right\} \epsilon_z \quad (11)$$

The second term in Equation 11 describes the effect of temperature on the optical fiber. When the temperature changes, two things happen that cause the Bragg condition to change: first, thermal expansion changes the distance between the grating planes; and second, the ERI changes, which causes the light wave's optical path to change. The second factor is the main contributor to the shift of the Bragg wavelength. This fragmentary contribution to the resonant wavelength shift can be written as:

$$\Delta\lambda_{BG} = \lambda_{BG}(\alpha_{\Lambda} + \alpha_n)\Delta T \tag{12}$$

From where you can easily get the temperature sensitivity of our grating:

$$\frac{\Delta\lambda_{BG}}{\Delta T} = \lambda_{BG}(\alpha_{\Lambda} + \alpha_n) \tag{13}$$

Where α_{Λ} is the thermal expansion coefficient, α_n is the thermo-optical coefficient.

Typical values of these parameters for an optical fiber: $\alpha_{\Lambda} = 0,55 \cdot 10^{-6}$ for fused silica, $\alpha_n = 8,6 \cdot 10^{-6}$ for an optical fiber doped with germanium.

Let us consider the effect of temperature on the spectral characteristics of a fiber Bragg grating. Equation 12 describes the impact of temperature on the optical fiber.

To accomplish this task, a setup was assembled that shows the effect of temperature in various ranges on the spectral characteristics of fiber Bragg gratings.

The error of the temperature measuring device does not exceed ± 0.5 °C at temperatures in the range of 18°C to 135°C. Also, this bench can carry out tests at low temperatures. This can be done with liquid nitrogen and a heating element. A resistive heating plate heats the grates. The size of the heating surface is 47cm×19 cm. an autotransformer provides temperature control. Environmental conditions:

- Operating temperature: from +5 to +40 °C;
- Storage temperature: from -5 to +40 °C;
- Humidity max 70% relative humidity.

The study was carried out on three Bragg gratings, which differ from each other in λ_{BG} .

On the basis of the obtained measurements, the spectral characteristics were constructed, and the values of the Bragg wavelength for each temperature value were obtained. Based on this, a plot of the Bragg wavelength was obtained from the temperature. An analysis of the diagrams shows that the value of the Bragg wavelength increases with increasing temperature, as evidenced by the measurement results in Table 1.

Table 1.
Bragg wavelengths as a function of a given temperature.

λ_B [nm]	1527,83	1528,022	1528,022	1528,117	1528,143	1528,242	1528,243	1528,3	1528,369	1528,42	1528,49	1528,527	1528,582	1528,608	1528,675	1528,733	1528,778	1528,82	1528,877	1528,955	1529,005	1529,093	1529,097
T [°C]	18	30	35	40	45	50	55	60	65	70	75	80	85	90	95	100	105	110	115	120	125	130	135

Figure 3 illustrates an experimental bench for temperature measurement and extension of an overhead power line cable.

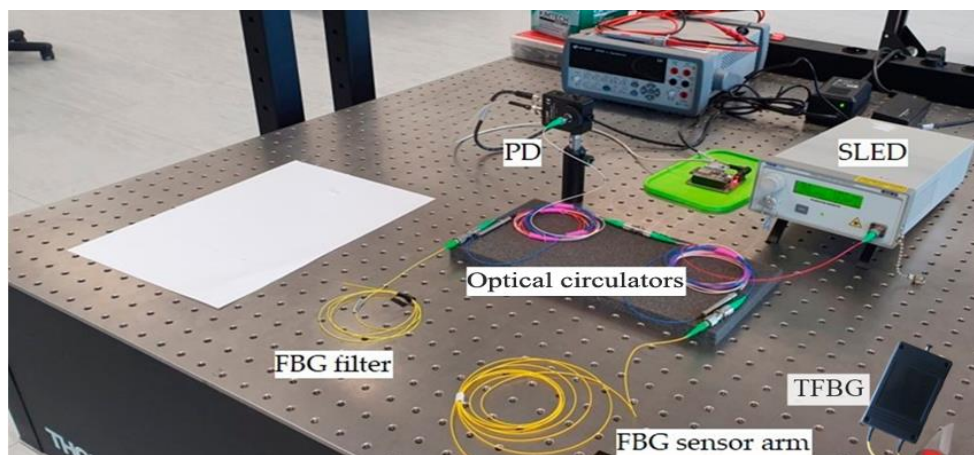


Figure 3.
Experimental stand for temperature measurement and cable extension of an overhead power line. SLED: super luminescent light-emitting diode; PD: photodetector.
Note: PD- Power delivery, SLED- LED spectral illumination, FBG filter- Fiber-optic sensor filter, FBG sensor arm- Fiber Optic sensor arm, TFBG- Fiber-optic sensor with inclined Bragg grating.

Figure 4 illustrates the outdoor test bench.

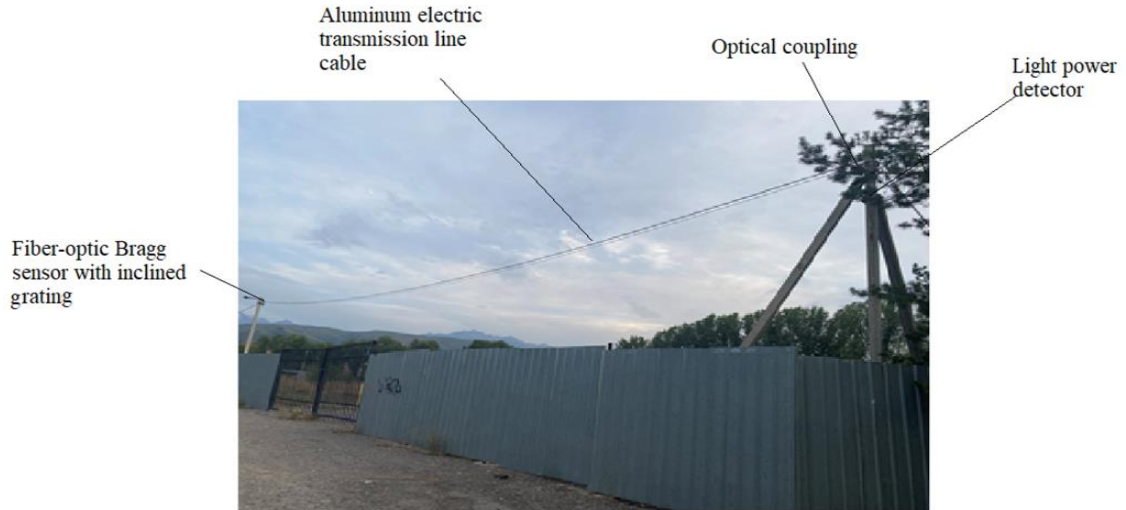


Figure 4. Outdoor test bench.

Figure 5 shows the spectral characteristics of tilted Bragg gratings.

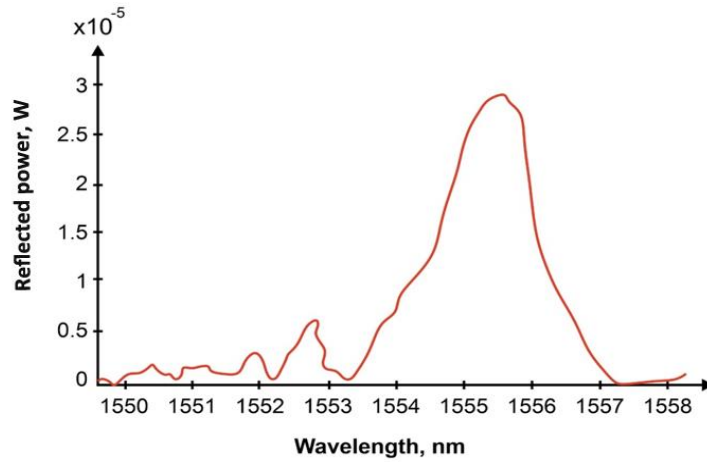


Figure 5. Spectral characteristics of tilted Bragg gratings.

Figure 6 shows the spectral response obtained using an optical spectrum analyzer and the system's transient response, allowing you to understand the significance of the voltage of the photodetector produces. The ranges shown in Figure 7 were measured using OSA with the appropriate transient response acquired using a photodetector.

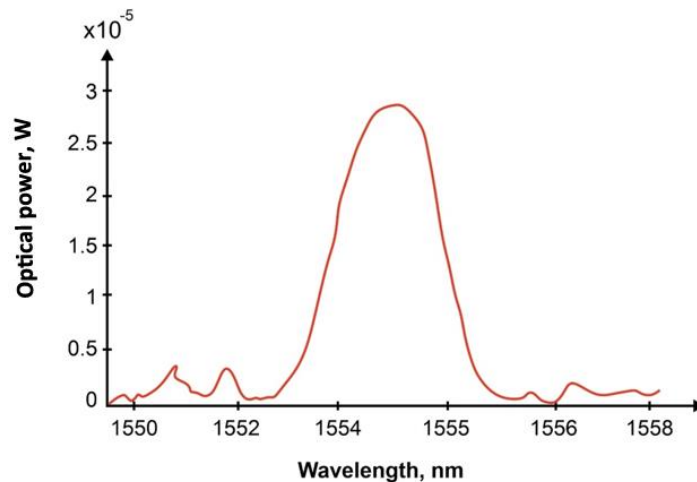


Figure 6. Spectral characteristics measured through an optical spectrum analyzer.

Figures 7 and 8 show the characteristics obtained using experimental measurements. The nature of changes in the optical range is similar, but there are differences in the spectral characteristics of the sensor and filter. Therefore, the processing characteristics are different. A particularly significant problem here is the fairly small spectrum of voltage changes at the photodetector. In the case of the systems used, the normalized significance of the voltage varies in the range of 0.52–1.93 V.

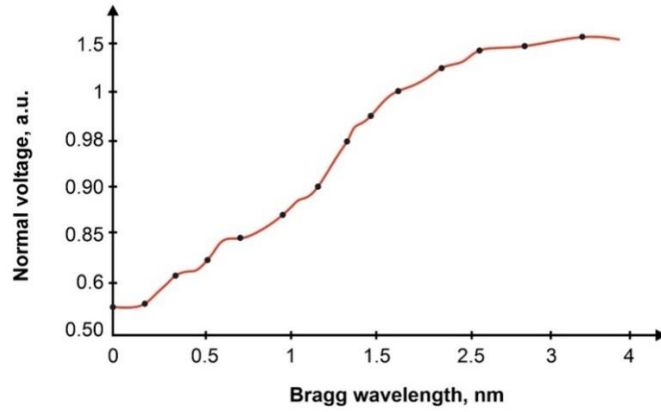


Figure 7.
Normal voltage as a function of wavelength.

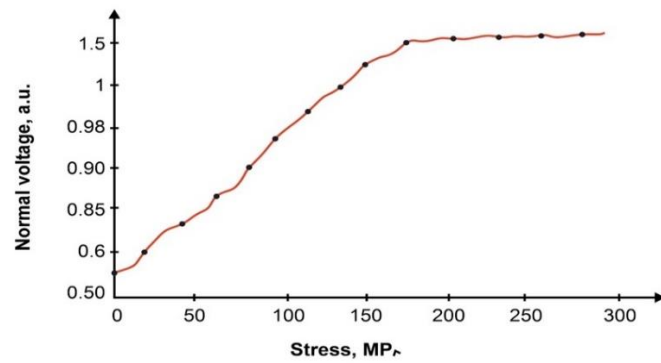


Figure 8.
Normal stress versus stress.

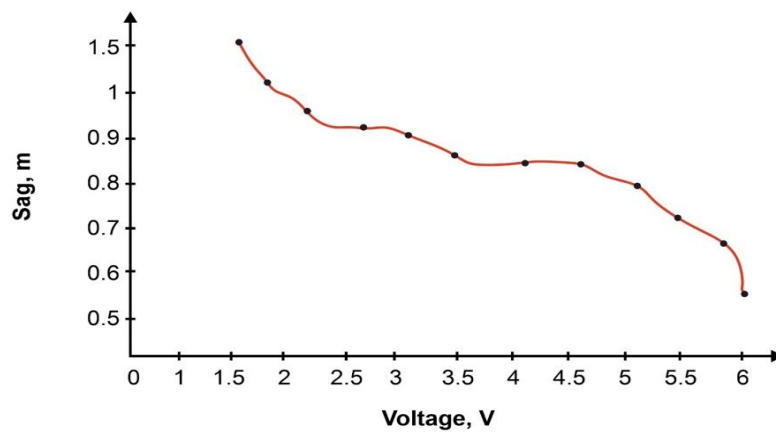


Figure 9.
The results of determining the amount of sag of the power line depending on the voltage measured by the photodetector for the power line.

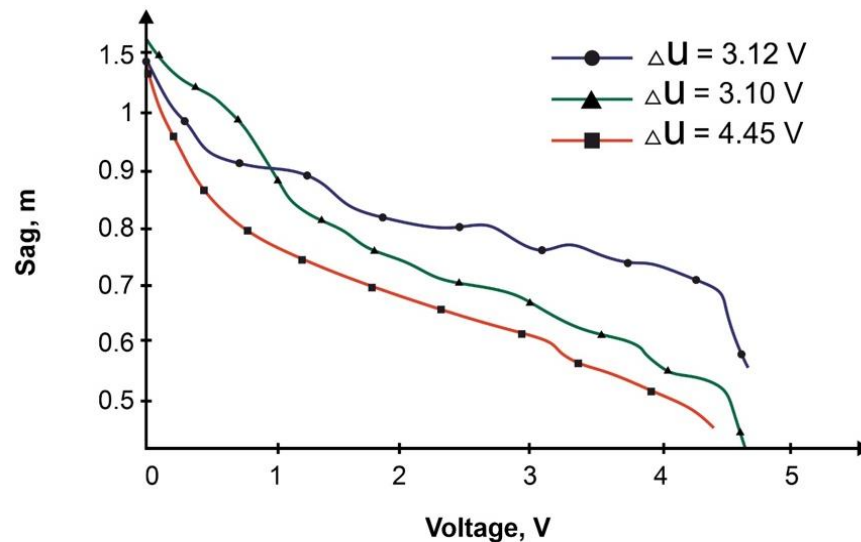


Figure 10. Results of determining the amount of sag of a power line depending on various voltages.

Figures 9 and 10 demonstrate that the voltage change detected by the photodetector increases noticeably in the case of straight spans of power transmission lines, independent of the spacing between the poles in the span. Working with a 50m galvanic current wire caused a change in the voltage that the photodetector measured after passing through the system. During the measurements, the temperature of the power line cable was in the range of 10-60 °C. This led to the extension of the test cable from 38.987 m to 49.275 m, the error was within 4%. It should be added that the deviation was measured using a fiber-optic sensor with an inclined grid. This sensor is sensitive to electromagnetic interference, and its use in measuring the condition of power lines can lead to incorrect results. It seems that at higher temperatures, which activate the impressive quality of sagging, the error can increase even by more than 8% or 10%.

4. Conclusions

In this study, which included a certain application of a fiber-optic sensor in the electric power industry, the result was an increase in the performance of electricity transmission and an increase in reliability. The results presented in this article may be the conclusion of the difficulty of mental and effective management of the power system. The constructed design for simulating the sagging of power transmission lines recommended in this article can be useful for the maintenance of power transmission and distribution lines, reducing capacity with appropriate control, increasing the productivity of the electric network, and achieving higher energy efficiency, as well as for calculating investments in energy infrastructure and large-scale energy sources. That part of the experiment used a fiber-optic sensor with an inclined Bragg lattice, which shows a small shift in the spectra. It was found that the transient property has a rectilinear characteristic associated with the main Bragg peak and a nonlinear spectrum covering the saturation slope associated with side bands on the narrower side. The study showed that by giving preference to the mechanical parameters of the elongation converter and the optical adjustment parameters, the optical-mechanical state can be adapted to the required range of deviation observation. The range of the difference depends on the distance between the poles and the appropriate length of the power line cable.

References

- [1] J. Zygarlicki and J. Mroczka, "Variable-frequency Prony method in the analysis of electrical power quality," *Metrology and Measurement Systems*, vol. 19, no. 1, pp. 39-48, 2012. <https://doi.org/10.2478/v10178-012-0003-1>
- [2] V. V. Terzija and V. Stanojevic, "STLS algorithm for power-quality indices estimation," *IEEE Transactions on Power Delivery*, vol. 23, no. 2, pp. 544-552, 2008. <https://doi.org/10.1109/tpwrd.2008.919312>
- [3] C. R. Black and W. A. Chisholm, "Key considerations for the selection of dynamic thermal line rating systems," *IEEE Transactions on Power Delivery*, vol. 30, no. 5, pp. 2154-2162, 2014. <https://doi.org/10.1109/tpwrd.2014.2376275>
- [4] V. Lovrenčić, M. Gabrovšek, M. Kovač, N. Gubeljak, Z. Šojat, and Z. Klobas, "The contribution of conductor temperature and sag monitoring to increased capacities of overhead lines (OHLs)," *Periodica Polytechnica Electrical Engineering and Computer Science*, vol. 59, no. 3, pp. 70-77, 2015. <https://doi.org/10.3311/ppce.8585>
- [5] Conductor Working Group P738, "IEEE 738-2012 standard for calculating the current-temperature relationship of bare overhead conductors—corrigendum 1." Piscataway, NJ, USA: IEEE Standards Association, 2013, pp. 1–10.
- [6] CIGRE Working Group 22.12, *Thermal behaviour of overhead conductors; CIGRE- international council on large electric systems*. Paris, France: 21 RUE D'ARTOIS, 2002.
- [7] P. Ramachandran, V. Vittal, and G. T. Heydt, "Mechanical state estimation for overhead transmission lines with level spans," *IEEE Transactions on Power Systems*, vol. 23, no. 3, pp. 908-915, 2008. <https://doi.org/10.1109/tpwrs.2008.926093>
- [8] M. Wydra, P. Kubaczynski, K. Mazur, and B. Ksiezopolski, "Time-aware monitoring of overhead transmission line sag and temperature with LoRa communication," *Energies*, vol. 12, no. 3, pp. 1-23, 2019. <https://doi.org/10.3390/en12030505>
- [9] C. Kaczmarek, "Properties of a fibre optic strain sensor in the configuration of a Mach-Zehnder modal interferometer with a polarization maintaining photonic crystal fibre," *Metrology and Measurement Systems*, vol. 25, no. 2, pp. 417-424, 2018.

- [10] P. Kisała, S. Ciężczyk, K. Skorupski, P. Panas, and J. Klimek, "Rotation and twist measurement using tilted fibre Bragg gratings," *Metrology and Measurement Systems*, vol. 25, pp. 429-440, 2018. <https://doi.org/10.24425/123893>
- [11] P. Kisała, J. Mroczka, S. Ciężczyk, K. Skorupski, and P. Panas, "Twisted tilted fiber Bragg gratings: New structures and polarization properties," *Optics Letters*, vol. 43, no. 18, pp. 4445-4448, 2018. <https://doi.org/10.1364/ol.43.004445>
- [12] M.-Y. Liu, S.-G. Zhou, H. Song, W.-J. Zhou, and X. Zhang, "A novel fibre Bragg grating curvature sensor for structure deformation monitoring," *Metrology and Measurement Systems*, vol. 25, pp. 577-587, 2018. <https://doi.org/10.24425/123899>
- [13] P. Kisała, D. Harasim, and J. Mroczka, "Temperature-insensitive simultaneous rotation and displacement (bending) sensor based on tilted fiber Bragg grating," *Optics Express*, vol. 24, no. 26, pp. 29922-29929, 2016. <https://doi.org/10.1364/oe.24.029922>
- [14] Z. Ding, Z. Tan, X.-X. Su, and D. Cao, "A fast interrogation system of FBG sensors based on low loss jammed-array wideband sawtooth filter," *Optical Fiber Technology*, vol. 48, pp. 128-133, 2019. <https://doi.org/10.1016/j.yofte.2019.01.004>
- [15] Y. Li *et al.*, "A highly precise FBG sensor interrogation system with wavemeter calibration," *Optical Fiber Technology*, vol. 48, pp. 207-212, 2019. <https://doi.org/10.1016/j.yofte.2019.01.006>
- [16] M. Maheshwari, Y. Yang, T. Chaturvedi, and S. C. Tjin, "Chirped fiber Bragg grating coupled with a light emitting diode as FBG interrogator," *Optics and Lasers in Engineering*, vol. 122, pp. 59-64, 2019. <https://doi.org/10.1016/j.optlaseng.2019.05.025>
- [17] C. Crunelle, M. Wuilpart, C. Caucheteur, and P. Mégret, "Original interrogation system for quasi-distributed FBG-based temperature sensor with fast demodulation technique," *Sensors and Actuators A: Physical*, vol. 150, no. 2, pp. 192-198, 2009. <https://doi.org/10.1016/j.sna.2008.11.018>
- [18] K. Liu *et al.*, "Investigation of PZT driven tunable optical filter nonlinearity using FBG optical fiber sensing system," *Optics Communications*, vol. 281, no. 12, pp. 3286-3290, 2008. <https://doi.org/10.1016/j.optcom.2008.02.034>
- [19] G. D. Lloyd, L. A. Everall, K. Sugden, and I. Bennion, "Resonant cavity time-division-multiplexed fiber Bragg grating sensor interrogator," *IEEE Photonics Technology Letters*, vol. 16, no. 10, pp. 2323-2325, 2004. <https://doi.org/10.1109/lpt.2004.834849>
- [20] M. Wydra, P. Kisała, D. Harasim, and P. Kacejko, "Overhead transmission line sag estimation using a simple optomechanical system with chirped fiber bragg gratings. Part 1: Preliminary measurements," *Sensors*, vol. 18, no. 1, p. 309, 2018. <https://doi.org/10.3390/s18010309>
- [21] A. L. Ribeiro, L. Ferreira, J. Santos, and D. A. Jackson, "Analysis of the reflective-matched fiber Bragg grating sensing interrogation scheme," *Applied Optics*, vol. 36, no. 4, pp. 934-939, 1997. <https://doi.org/10.1364/ao.36.000934>
- [22] M. Davis and A. Kersey, "Matched-filter interrogation technique for fibre Bragg grating arrays," *Electronics Letters*, vol. 31, no. 10, pp. 822-823, 1995. <https://doi.org/10.1049/el:19950547>
- [23] S. A. Wade, D. P. Attard, and P. R. Stoddart, "Analysis of transmission mode of a matched fiber Bragg grating interrogation scheme," *Applied Optics*, vol. 49, no. 24, pp. 4498-4505, 2010. <https://doi.org/10.1364/ao.49.004498>
- [24] M. A. Casas-Ramos and G. E. Sandoval-Romero, "Strain detection and measurement using a matched fibre Bragg grating," *Journal of Electromagnetic Waves and Applications*, vol. 32, no. 12, pp. 1519-1526, 2018. <https://doi.org/10.1080/09205071.2018.1446366>
- [25] R. Fallon, L. Zhang, A. Gloag, and I. Bennion, "Identical broadband chirped grating interrogation technique for temperature and strain sensing," *Electronics Letters*, vol. 33, no. 8, pp. 705-707, 1997. <https://doi.org/10.1049/el:19970486>
- [26] H. Zhang, J. Jiang, S. Liu, H. Chen, X. Zheng, and Y. Qiu, "Overlap spectrum fiber Bragg grating sensor based on light power demodulation," *Sensors*, vol. 18, no. 5, p. 1597, 2018. <https://doi.org/10.3390/s18051597>
- [27] G. Wild and S. Richardson, "Numerical modeling of intensity-based optical fiber Bragg grating sensor interrogation systems," *Optical Engineering*, vol. 52, no. 2, pp. 024404-024404, 2013. <https://doi.org/10.1117/1.oe.52.2.024404>
- [28] L. A. Garção *et al.*, "Temperature compensation method for FBG-based current sensors for transmission lines," in *In Proceedings of the IEEE International Instrumentation and Measurement Technology Conference (I2MTC), Houston, TX, USA, 14-17 May, 2018*, pp. 1-6.